A Lattice Model for the Simulation of Diffusion in Heterogeneous Polymer Systems. Simulation of Apparent Diffusion Constants as Determined by Pulse-Field-Gradient Nuclear Magnetic Resonance

Guoxing Lin, Jinghui Zhang, Haihui Cao, and Alan A. Jones*

Carlson School of Chemistry and Biochemistry, Clark University, Worcester, Massachusetts 01610

Received: December 18, 2002; In Final Form: April 8, 2003

The diffusion of molecules through heterogeneous media is not simple Fickian diffusion on the length scale of the heterogeneities. Pulse-field-gradient (PFG) NMR measurements of diffusion reflect this by yielding apparent diffusion constants that are dependent on the time over which diffusion is observed. Equations for simple cases of tortuous diffusion and restricted diffusion are available where some fraction of the medium is assumed to be permeable and some fraction is impermeable. In many polymer systems, the medium has domains that are more permeable and less permeable. In the limit of long times and above the percolation threshold, diffusion in such systems can be characterized with effective medium theory (EMT). To characterize diffusion as a function of time in heterogeneous media and at all compositions, a lattice model is presented based on an approach developed by Ediger. The lattice model gives results that match EMT at long times and produces tortuous and restricted diffusion above and below the percolation limit when one domain is made impenetrable. It also shows a wide range of behavior of the apparent diffusion constant, relative to observation time, which is intermediate between tortuous diffusion and restricted diffusion. The intermediate behavior arises for various ratios of the diffusion constant in the more- and less-permeable domains and for various ratios of solubility between the more- and less-permeable domains. Brief comparisons are made with PFG NMR data on a heterogeneous, high-permeability copolymer and on a polymer blend composed of more- and less-permeable constituents. The model demonstrates that apparent diffusion data from PFG NMR provide a new structural view of the heterogeneities in systems with more- and less-permeable domains.

Introduction

Diffusion of low-molecular-weight penetrants in a polymer can be quantitatively characterized using pulse-field-gradient (PFG) NMR experiments.[1] These experiments determine the self-diffusion constant in cases where simple Fickian diffusion is observed to occur in a homogeneous matrix typically over length scales of micrometers. An example of such a system is toluene in poly(isobutylene) above the glass transition, where the toluene is uniformly distributed in the polymer.[2−4] There are heterogeneities in glassy polymers on the length scale of a few nanometers,[5,6] but these would be averaged in a typical PFG NMR experiment. On the other hand, polymer systems can be heterogeneous on a larger length scale than nanometers for many reasons, including partial crystallinity, blending, copolymerization, and the addition of fillers. The heterogeneity leads to more-complex diffusion and a frequent result is that the apparent diffusion constant is dependent on the length scale over which diffusion is observed in the PFG NMR experiment.[1,7−9] Figure 1 shows a simple form of the three pulse stimulated echo sequences commonly used for diffusion determinations and the time scale over which diffusion is observed is determined by the value of Δ (as defined in Figure 1) in the pulse sequence.

Perhaps the simplest polymeric example to understand is a semicrystalline polymer where diffusion occurs in the amorphous component while the crystalline component is impenetrable. In this case, diffusion is impeded by the crystalline phase. The penetrant can be considered to undergo a random walk through the amorphous domain; however, when it reaches the surface of a crystallite, the penetrant will be reflected. This will lead to a slowing of diffusion, relative to a system that is completely amorphous. If diffusion is observed at small values of Δ in the PFG NMR experiment, few crystallites will be encountered by the penetrant and the diffusion constant will be similar to that observed in a completely amorphous system. As the value of Δ increases, penetrant molecules will encounter the impenetrable crystallites more frequently and diffusion will apparently slow. At sufficiently long times, the diffusion constant will become constant after the length scale is sufficiently long so that averaging over the morphological structure

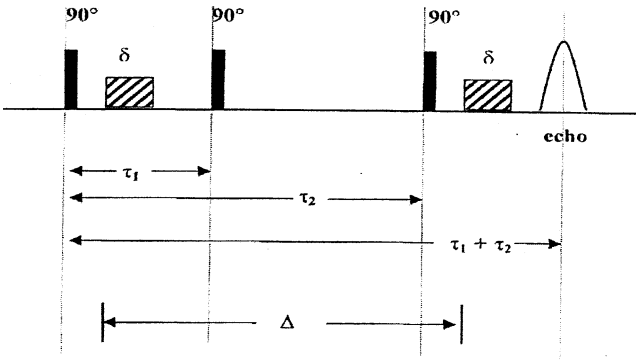

Figure 1. Pulse-field-gradient (PFG) stimulated echo sequence. The time over which diffusion occurs is denoted as Δ.

* Author to whom correspondence should be addressed. E-mail: ajones@clarku.edu.

10.1021/jp022619o CCC: $25.00
Published on Web 05/30/2003

occurs. The ratio given by the diffusion constant observed at short times or in a completely amorphous system divided by the value at long times is called the tortuousity, α, and this serves as a measure of the increase in obstructions encountered by the diffusing penetrant.

There are descriptions of tortuous systems produced by the presence of impenetrable regions.[7−9] However, in a polymeric system such as a blend or a copolymer, there may be differences in translational mobility in different spatial regions but both regions are penetrable. Thus, diffusion could be fast in one region and slow in the other region. For a case such as this, we are not aware of a model that can predict the apparent diffusion constant, D_{app}, at different times, as would be observed in a PFG NMR experiment.

To improve our understanding of such systems, we are proposing a two-domain simulation model that allows for spatial heterogeneity. This simulation model is based on a model presented by Ediger et al.,[10] which was developed to clarify the physical basis for the apparent enhancement of translational diffusion, relative to rotational motion in glasses. Results of the simulation at large values of Δ, where the value of D_{app} becomes constant, can be compared to effective medium theory (EMT).[10−12] The simulation will also give the dependence of D_{app} on Δ, which is not given by the theory. The simulation also can provide results below the percolation limit where EMT is not applicable and in cases where the difference between fast and slow diffusion is small.

Simulation results can also be compared to simple models for tortuous[7−9] and restricted diffusion,[1] where diffusion is impeded by impenetrable domains. While the value of D_{app} decreases to a plateau value as Δ increases for tortuous diffusion, the value of D_{app} continually decreases as Δ increases for restricted diffusion. These predictions can be compared to the simulation results for cases where the regions impeding diffusion are penetrable but less penetrable than the other domain. Reduced penetration can be produced either by changing solubility or by changing the diffusion constant in one of the domains.

The other key parameter in the problem is the morphological characteristics of the two regions of differing permeability. In this report, a random dispersion of regions supporting fast diffusion and slow diffusion will be considered. Other morphologies will be considered in the future. The size, a, of the regions is also a relevant consideration and the effect of this parameter scales with the diffusion constant, D, according to the ratio D/a^2.

Brief qualitative comparisons of the simulation results will be made to two sets of data, although the main objective of this report is the development of the simulation model for heterogeneous diffusion. The first comparison will be for PFG measurements on pentane in the copolymer of tetrafluoroethylene (TFE) and 2,2-bis(trifluoromethyl)-4,5-difluoro-1,3-dioxole (PDD)[13−15] and the second will be for PFG measurements on diethyl ether in a blend of poly(methyl methacrylate) (PMMA) with poly(ethylene oxide) (PEO). In both cases, D_{app} is dependent on Δ.

Experimental Section

PFG measurements were made on a Varian Inova 400 MHz wide-bore NMR spectrometer either in a $^1H(^{15}N-^{31}P)$ 5-mm PFG indirect detection probe, by observing proton signals from the penetrant, or in an 8-mm direct detection probe with high gradient capability (1000 G/cm) from Doty Scientific. Samples were prepared by adding the appropriate amount of penetrant to either a cast film of TFE/PDD or PEO/PMMA. The first sample was 8 wt % pentane in AF 1600 (DuPont), and the second sample was 10% diethyl ether in a 20 wt % blend of PEO in PMMA. Each sample was then sealed in a 5-mm NMR tube. AF 1600 is composed of 65% PDD and 35% TFE. The TFE/PDD films were cast from a perfluoroheptane solution of the copolymer and dried to constant weight in a vacuum oven at 50 °C. The PEO/PMMA blend was cast from benzene and also dried in a vacuum oven. The TFE/PDD copolymers were provided by DuPont. The PEO and PMMA were purchased from Scientific Polymer Products, Incorporated. For PEO, the molecular weight (M_w) is 5×10^6; for PMMA, $M_w = 7.5 \times 10^3$.

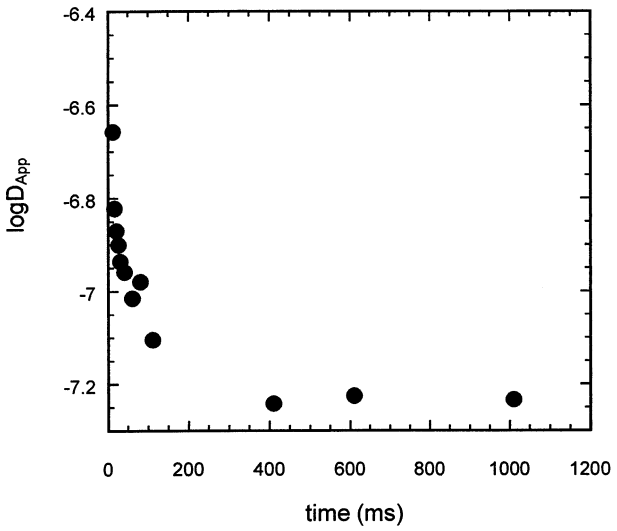

Figure 2. Logarithm of D_{app} versus time (or Δ) for pentane in the copolymer tetrafluoroethylene/2,2-bis(trifluoromethyl)-4,5-difluoro-1,3-dioxole (TFE/PDD).

The apparent diffusion constant of the penetrant, D_{app}, was measured as a function of the time Δ over which self-diffusion occurs in the stimulated echo pulse sequence shown in Figure 1. Only the initial decay of echo amplitude was monitored, typically to a level of ∼50% of the original amplitude. At a given time Δ, the quantity $q = \gamma\delta g/2\pi$ was varied by changing the gradient amplitude, g, from 0 to 60 G/cm for the indirect probe and from 0 to 800 G/cm for the Doty probe. The time Δ ranged from 2 ms to 1 s. A fixed value of δ, which is the length of the gradient pulses (1−8 ms), was used for a given determination of the apparent diffusion constant. The value of D_{app} at a given value of Δ is calculated from the slope of a plot of the logarithm of the echo amplitude versus g^2.

Results for pentane in TFE/PDD are shown in Figure 2, and similar data on diethyl ether in the PEO/PMMA blend are shown in Figure 3.

The Simulation Model

The simulation is performed on a cubic lattice that is divided into blocks of two types: one that supports fast diffusion and one that supports slow diffusion. The two types of blocks or domains are distributed randomly on the lattice. Diffusion inside a block is homogeneous. A block consists of 8000 cubes ($20 \times 20 \times 20$) and the entire lattice consists of 8000 blocks or 64×10^6 cubes. Periodic boundary conditions are used. In our approach, there is no exchange of fast and slow blocks as a function of time, although this was allowed in the original model by Ediger et al.[10] Because the systems currently of interest are glasses well below the glass transition, no time-dependent exchange of block character is likely.

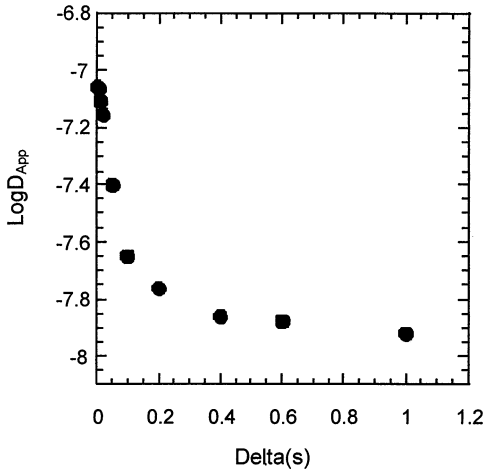

Figure 3. Logarithm of D_{app} versus time (or Δ) for diethyl ether in a blend of poly(ethylene oxide) (PEO) and poly(methyl methacrylate) (PMMA) that is 20 wt % poly(ethylene oxide).

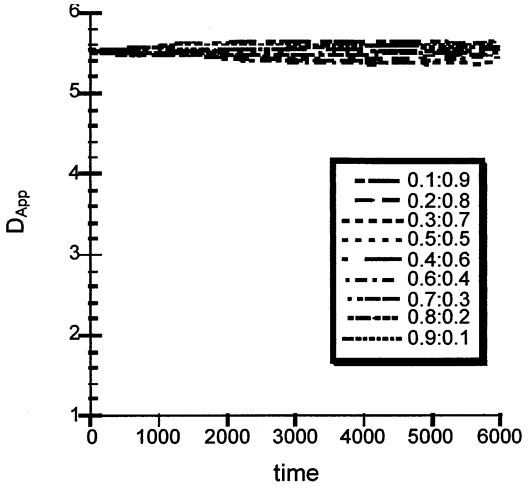

Figure 4. Plot of the apparent diffusion constant D_{app} versus time, where D_{app} is simulated as a function of time for different compositions of fast and slow domains but $D_{fast} = D_{slow}$ ($D_{slow}/D_{fast} = 1$) for all compositions.

To simulate diffusion, random walks are performed on the cubic lattice through both the blocks that support either fast or slow diffusion. Typically, 2000−3000 walks are performed to obtain D_{app} as a function of time and each walk begins with a random choice of the starting point on the lattice. For the cases of differing solubility between the two types of blocks, the starting points are weighted, according to the relative solubility. An apparent diffusion constant is calculated at various times or equivalently after a certain number of steps, based on an average over the 2000 or 3000 individual walks.

Following Ediger et al.,[10] the diffusion rate in a block is set by specifying a jump rate k_{ij} for a jump from the ith cube to the jth cube. Only jumps to the six nearest neighbors are considered. The average time to leave site i is

$$\tau_{jump} = \frac{1}{\sum_j k_{ij}} \tag{1}$$

If i and j are in a block of the same type, the time scale is set by

$$k_{ij} = \frac{1}{18\tau} \tag{2}$$

where τ is the rotational correlation time. If this is within the block supporting fast diffusion, then we will also write $k_{ij} = k_{fast-fast}$ with a similar notation for motion within the slow block. If i and j are in blocks of two different types (at the interface between fast and slow regions) and the solubility, S, of the penetrant is uniform ($S_{fast} = S_{slow}$), then

$$k_{ij} = \frac{1}{2\left(\frac{1}{18\tau_{fast}} + \frac{1}{18\tau_{slow}}\right)} = \frac{(k_{fast-fast} + k_{slow-slow})}{2} \tag{3}$$

If the solubilities S_{slow} and S_{fast} are different in the slow and fast blocks, then

$$\frac{S_{slow}}{S_{fast}} = R \neq 1 \tag{4}$$

Solubility can be related to exchange rates using microreversibility.

$$S_{slow}k_{slow-fast} = S_{fast}k_{fast-slow} \tag{5}$$

$$Rk_{slow-fast} = k_{fast-slow}$$

A relationship between the exchange rates within blocks to the exchange rates between blocks must also be specified. Arbitrarily,

$$\frac{k_{slow-slow} + k_{fast-fast}}{2} = \frac{k_{slow-fast} + k_{fast-slow}}{2} \tag{6}$$

Mean square displacements are actually produced by averaging over 2000−3000 walks and apparent diffusion constants are calculated from the relationship

$$D_{app}(t) = \frac{\langle r^2 \rangle}{6t} \tag{7}$$

Simulation Results

To check the simulation, a homogeneous lattice was produced by setting $k_{fast-fast} = k_{slow-slow}$, so that $D_{fast} = D_{slow}$. If τ is set equal to 10^{-2}, then $\tau_{jump} = 3 \times 10^{-2}$ and $k_{ij} = 5.56$. After n jumps, $t = 3n \times 10^{-2}$ and $\langle r \rangle = nl^2$, so $D_{app}(t) = (nl^2)/(18n\tau)$. If l, the step size or lattice size, is set to unity, then $D_{app} = 5.56$ at all times on this homogeneous lattice. Note that, in the work by Ediger et al., $\tau = 1$, so $D = 0.0556$.

The machinery of a heterogeneous lattice was used to make predictions of D_{app} as a function of time and the fraction of fast and slow blocks, but the diffusion rates were equal in all blocks. The results are shown in Figure 4, and the value of D_{app} is found to be equal to 5.56 for all times and all fractions of fast and slow blocks, with an error of ±5%. This is the expected result.

Now, predictions can be made from this simulation model for different ratios of D_{fast} to D_{slow}, different fractions of fast and slow blocks, and different solubilities. Figure 5 shows plots of $\langle r^2 \rangle/6$ versus time for systems that are composed of 10% fast blocks and 90% slow blocks for different ratios of D_{fast} to D_{slow}. In the test case where $D_{fast} = D_{slow}$, the quantity $\langle r^2 \rangle$ increases linearly with time, as it should, whereas the results for other ratios of D_{fast} to D_{slow} shown in Figure 5 are more complicated. As D_{slow} decreases, the slopes of the plots of $\langle r^2 \rangle$

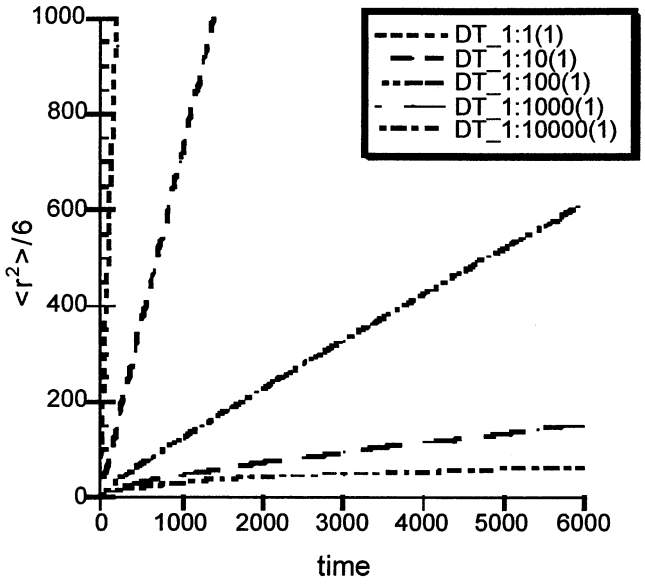

Figure 5. Average square of the distance, divided by 6, versus time for a lattice that is composed of 10% fast and 90% slow domains. The ratio of D_{slow} to D_{fast} changes from 1 to 10^{-4}.

decrease as time increases. The slope is proportional to D_{app}; therefore, this observation corresponds to decreases in the effective diffusion coefficient D, which is similar to the behavior observed in heterogeneous materials in the PFG experiment.

Figure 6 presents plots of log D_{app} versus time for a range of compositions of fast and slow blocks. In this example, $D_{fast}/D_{slow} = 100$ and $D_{fast} = 5.56$, as will be the case in all examples. When the fraction of the lattice that represents the fast component is >0.33, D_{app} decreases to a plateau value. Note that, although the block length is 20, a time of ~1000 (or 3.3×10^4 fast jumps or 3.3×10^2 slow jumps) is required to reach the plateau value of D_{app} for a composition of 40% fast blocks. Thus, the effect of the domain structure persists over much longer length scales than the size of the blocks or domains used to construct the heterogeneous lattice. The value of 0.33 is the percolation limit, and the plateau value of D_{app} can be compared with EMT[11] for fast-block fraction values of >0.33. The relevant equation[11] is

$$D_{app} = D_{fast}\left[1.5\epsilon - 0.5 + \chi\left(1 - 1.5\epsilon + \frac{1}{3\epsilon - 1}\right)\right] \quad (8)$$

where $\chi = D_{slow}/D_{fast}$. Table 1 summarizes the comparisons with EMT for a range of compositions and values of the parameter χ. For $\chi < 0.01$ and fast-block compositions of >0.5, the comparisons between EMT and the simulations are within 5%. Discrepancies are observed for $\chi = 0.1$ and compositions near the percolation limit. These discrepancies arise from higher-order terms in χ, which are not included in eq 8. Aside from the expected limitations[11] of eq 8, the comparisons between the simulation and EMT are good.

For compositions with <0.33 fast blocks, the value of D_{app} decreases over the range of times studied. Qualitatively, this behavior is similar to restricted diffusion,[1] although, because the slow regions are permeable, albeit with reduced rates of diffusion, diffusion is not truly restricted. Cases with greater similarity to restricted diffusion will be considered later.

Figure 7 is similar to Figure 6, except the composition is 10% fast blocks and different ratios of D_{fast} to D_{slow} are used (from 1 to 10 000). For ratios ≥100, there is a continual decrease in D_{app} over the time range studied. This behavior is again

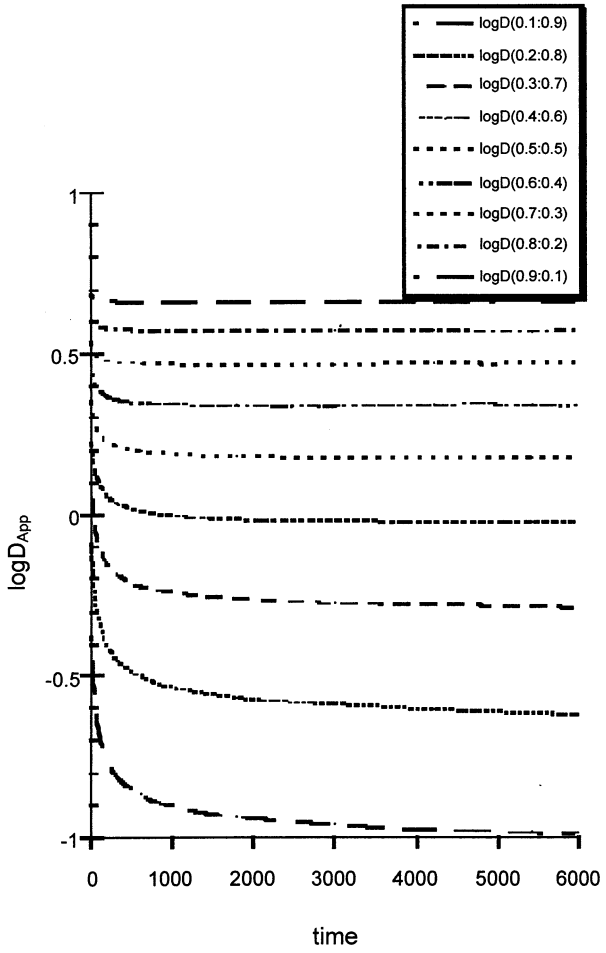

Figure 6. Plot of the apparent diffusion constant D_{app} versus time, where D_{app} is simulated as a function of time for different compositions of fast and slow domains and with $D_{slow}/D_{fast} = 10^{-2}$.

TABLE 1: Simulated Diffusion Constants at Time = 1000 (D_{app}), Compared with that from Effective Medium Theory (D_{EMT})

population, fast:slow	D_{EMT}	D_{app}
	$D_{Slow}/D_{Fast} = 1$	
0.5:0.5	5.5556	5.5219
	$D_{Slow}/D_{Fast} = 10^{-1}$	
0.4:0.6	3.5200	1.7176
0.5:0.5	2.6125	2.2287
0.6:0.4	2.9425	2.7301
0.7:0.3	3.4975	3.5017
0.8:0.2	4.1329	4.0629
0.9:0.1	4.8060	4.7153
	$D_{Slow}/D_{Fast} = 10^{-2}$	
0.4:0.6	0.84700	0.9444
0.5:0.5	1.4987	1.5015
0.6:0.4	2.2743	2.1700
0.7:0.3	3.0722	2.9392
0.8:0.2	3.8783	3.7240
0.9:0.1	4.6881	4.6058
	$D_{Slow}/D_{Fast} = 10^{-3}$	
0.4:0.6	0.57970	0.8815
0.5:0.5	1.3874	1.5184
0.6:0.4	2.2074	2.1375
0.7:0.3	3.0297	3.0765
0.8:0.2	3.8528	3.7894
0.9:0.1	4.6763	4.6706

qualitatively similar to restricted diffusion, which is reasonable because the slow diffusion is significantly reduced, relative to

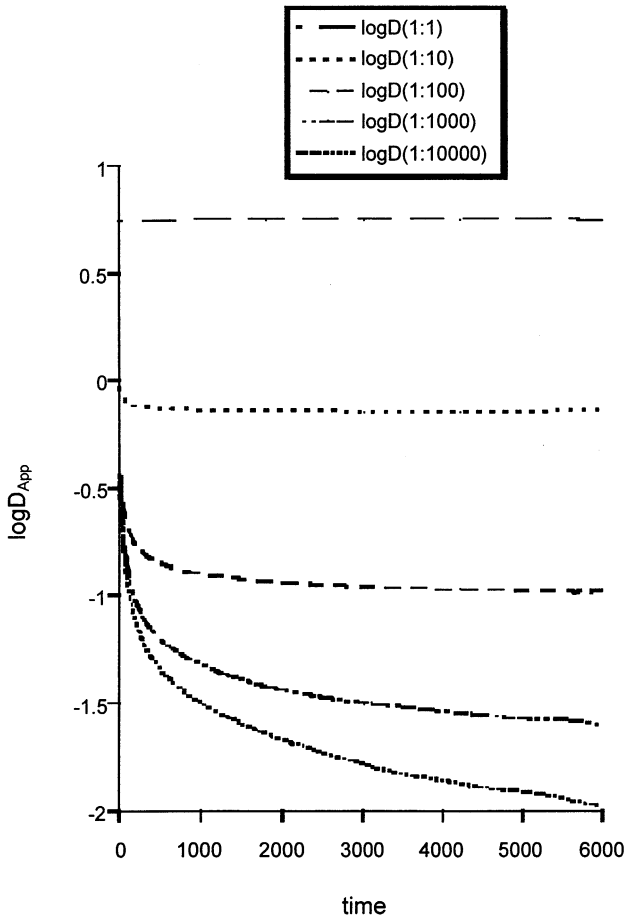

Figure 7. Plot of the apparent diffusion constant D_{app} versus time, where D_{app} is simulated as a function of time for a composition of 10% fast domains and ratios of D_{slow} to D_{fast} ranging from 1 to 10^{-4}.

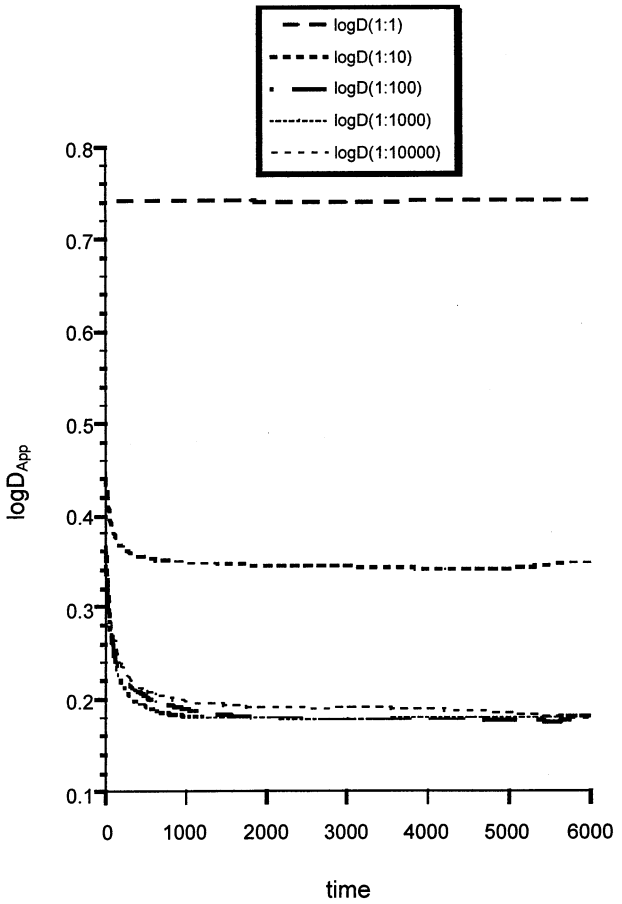

Figure 8. Plot of the apparent diffusion constant D_{app} versus time, where D_{app} is simulated as a function of time for a composition of 50% fast domains and ratios of D_{slow} to D_{fast} ranging from 1 to 10^{-4}.

the fast diffusion. For $D_{fast}/D_{slow} = 10$, D_{app} decreases to a plateau value, which is similar to tortuous diffusion, even though the composition is below the percolation limit. This is sensible, however, because the slow blocks support diffusion at a reasonable rate.

Figure 8 shows log D_{app} as a function of time for a composition with 50% fast blocks and D_{fast}/D_{slow} ratios of 1−10 000. In all cases, the behavior of D_{app} is qualitatively tortuous, except for a D_{fast}/D_{slow} ratio of 1, which is the case of simple diffusion. As the ratio increases from 100 to 10 000, there is little change in the plateau value. Thus, if D_{slow} is more than 2 orders of magnitude slower than D_{fast}, the slow domains appear impermeable, based on the time dependence, and the plateau value is almost independent of the actual value of D_{slow}.

Next, the effect of solubility will be considered. In all cases so far, solubility in the two blocks was equal and solubility throughout the lattice was uniform. In the following cases, a solubility difference is produced by weighting the starts of the walks and through the use of eqs 5 and 6. Figure 9 contains plots of log D_{app} versus time for a composition of 50% fast blocks and values of the solubility ratio R equal to 0.1, 0.01, and 1×10^{-6}. The ratio of D_{fast} to D_{slow} is 10 000. In these cases, the concentration in the slow block is small or near zero, and this is in combination with very slow diffusion. This is tending toward the case where the slow domains are impermeable, and this limit is essentially reached when R is set equal to 1×10^{-6}. This should give tortuous diffusion, which is seen in Figure 9, where D_{app} tends toward a plateau value. A considerable amount of time is required to reach the plateau, given that the block size for slow and fast blocks is $20 \times 20 \times 20$. Also, there is little change between $R = 1 \times 10^{-2}$ and $R = 1 \times 10^{-6}$, implying that a 100-fold decrease in solubility leads to effectively impermeable domains. For the composition of 50% fast blocks and $R = 1 \times 10^{-6}$, the plateau value of D is 1.6, which implies a tortuosity of $\alpha = 5.56/1.6 = 3.5$, which can be compared to the result for randomly packed spheres.[8]

A quantitative model based on diffusion through randomly packed impenetrable spheres can be compared to the results of randomly packed blocks simulated here. For the case of spheres, the equation for the apparent diffusion constant at a given value of Δ divided by the diffusion constant for the pure penetrant, D_0, is

$$\frac{D_{app}(\Delta)}{D_0} = 1 - \left(1 - \frac{1}{\alpha}\right)\left\{\frac{c\sqrt{\Delta} + \left(1 - \frac{1}{\alpha}\right)\frac{\Delta}{\Theta}}{\left(1 - \frac{1}{\alpha}\right) + c\sqrt{\Delta} + \left(1 - \frac{1}{\alpha}\right)\frac{\Delta}{\Theta}}\right\} \quad (9)$$

The tortuosity is represented by α, and c is given by the equation

$$c = \frac{4}{9\sqrt{\pi}}\left(\frac{S}{V}\right)\sqrt{D_0} \quad (10)$$

where (S/V) is the surface-to-volume ratio and Θ is given by

$$\Theta = 0.147\left(\frac{d^2}{D_0}\right) \quad (11)$$

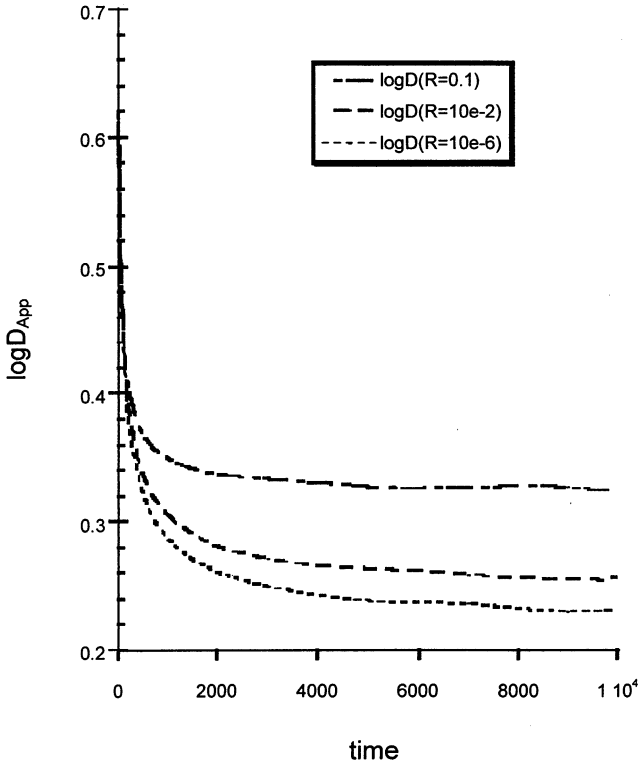

Figure 9. Plot of the apparent diffusion constant D_{app} versus time, where D_{app} is simulated as a function of time for a composition of 50% fast domains, with $D_{slow}/D_{fast} = 10^{-4}$, and three different solubilities R (0.1, 10^{-2}, and 10^{-6}).

For spherical bead packs, d is the diameter of the spheres. The surface-to-volume ratio is also related to d by

$$\frac{S}{V} = \frac{6\left(\frac{1}{\varphi} - 1\right)}{d} \tag{12}$$

where φ is the porosity. A very good fit of the simulation for $R = 0.1$ in Figure 9 is possible using the following parameters: $D_0 = 4.38$, $\alpha = 2.11$, $c = 0.048$, and $\theta = 48.8$. It should be kept in mind that the slow domains are not really impenetrable with $R = 0.1$ and a 10 000-fold difference in diffusion constants. At short times Δ, the quantity D_{app}/D_0 should be linear with the square root of Δ, according to eq 9, and a D_0 value of 4.38 is determined using this extrapolation procedure. This methodology treats the simulation results as if they were experimental data where D_0 might not be known. The true value of D_0 used in the simulation is 5.56, which gives some sense of the errors associated with applying this analysis. If the value of d is calculated from θ and D_0, the result is 38. If the sphere were inscribed inside the block, the result for d should be 20. Given all the differences between the two approaches, the discrepancy between 38 and 20 seems acceptable. Equation 9 also provides a good fit to the case where $R = 1 \times 10^{-6}$ with $\alpha = 2.95$, $D_0 = 4.93$, $c = 0.053$, and $\Theta = 98.2$. This yields a value of $d = 57$. Both the values of D_0 and d determined by applying eq 9 to the simulations would be useful information to characterize the system if the simulations were an experimental result, even though the results are only estimates of d. The large results for d are probably more-accurate estimates of the size of the objects impeding diffusion, because the impenetrable domains are composed of cubes with a dimension of 20. The cubes are allowed to touch in the construction of the overall structure; at a level of 50% impenetrable domains, they would touch, creating a larger structure.

Turning to a case where tortuous behavior is not expected, plots similar to Figure 9 are shown in Figure 10 for the case where only 10% of the blocks are fast. This fraction of fast domains is well below the percolation limit, so D_{app} continually decreases, as might be expected over the range of times shown. For $R = 0.1$ and 0.01, the system is not truly restricted, because the slow domains are permeable; however, the qualitative behavior is qualitatively restricted, because D_{app} continually decreases in Figure 10. However, a plot of $\langle r^2 \rangle$ in Figure 11 shows a continual increase instead of a plateau; a plateau would be expected for true restricted diffusion. A plateau is clearly reached for $R = 1 \times 10^{-6}$. Even for the larger values for R, there is however a drastic decrease in slope in Figure 11 as time increases, which is consistent with a significant impediment to diffusion over longer length scales. The plateau value of $\langle r^2 \rangle$ in Figure 11 for $R = 1 \times 10^{-6}$ is 360. Using the equation for diffusion restricted to a sphere,[1] the plateau value equals $a^2/5$, where a is the radius of the sphere. If the result for a sphere is applied to the plateau in Figure 11, $a = 8.5$. For a sphere inscribed in a cube, $2a$ corresponds to the side of the cube, which is 17. The side dimension of the fast domain in our lattice simulation is 20; therefore, the application of the equation for diffusion restricted to a sphere yields a result that is similar to the size scale used in the simulation. In the case of only 10% of the structure being fast domains, there is only a small chance of the fast domains touching, leading to a good estimate of the fast-domain size.

A fit of the entire simulation curve can be attempted, using an equation for the attenuation of signal intensity $E(q, \Delta)$ for diffusion restricted to a sphere.[13] The equation is given by

$$E(q,\Delta) = \frac{9[(\pi qd)\cos(\pi qd) - \sin(\pi qd)]^2}{(\pi qd)^6} + 6(\pi qd)^2 \sum_{n=0}^{\infty} [j_n'(\pi qd)]^2 \sum_m \frac{(2n+1)\alpha_{nm}^2}{\alpha_{nm}^2 - n^2 - n} \exp\left(-\frac{\alpha_{nm}^2 D\Delta}{(d/2)^2}\right) \frac{1}{[\alpha_{nm}^2 - (\pi qd)^2]^2} \tag{13}$$

where α_{nm} is the mth nonzero root of the equation $j_n'(\alpha_{nm}) = 0$ and j is the spherical Bessel function of the first type. Note that $q = (2\pi)^{-1}\gamma g\delta$, where δ is the gradient pulse length. For the case where $R = 10^{-6}$, a very good match of the simulated curve to this equation is achieved for a sphere of diameter $d = 30 \pm 2$ and $D_0 = 4.5 \pm 0.3$ for small q. Equation 13 was used to generate echo decay curves, as a function of q^2, which were matched to echo decay curves using D_{app} generated from the lattice simulation. For the cases of $R = 10^{-1}$ and 10^{-2}, this equation for diffusion restricted to a sphere does not match the plots of D_{app} versus time. These latter cases are not truly restricted diffusion, which is approached for $R = 10^{-6}$; therefore, the overall comparison between the theory and the simulation is acceptable. These values of d and D_0 are not very different than the parameters of the simulation where the block size is 20 and $D_0 = 5.56$.

Comparison to Experimental Results

The first set of experimental data to consider in Figure 2 is for pentane in the copolymer TFE/PDD. This is a very permeable polymer at temperatures well below the glass transition.[14−20] The fractional free volume in this high-perme-

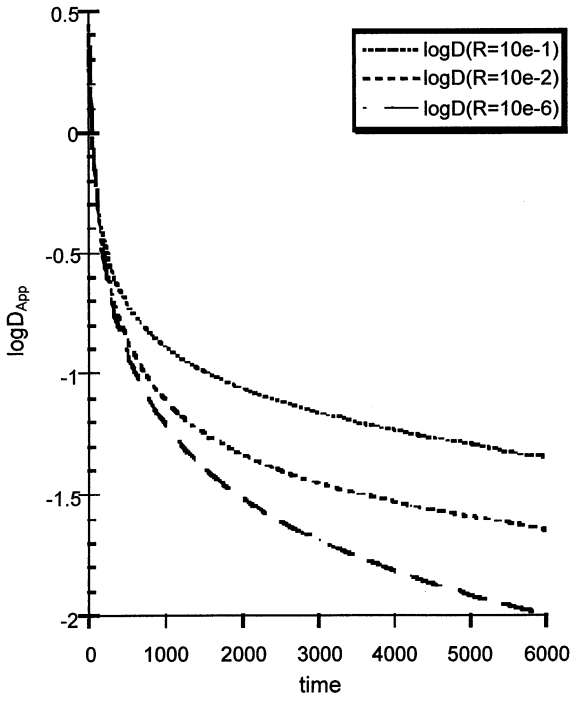

Figure 10. Plot of the apparent diffusion constant D_{app} versus time, where D_{app} is simulated as a function of time for a composition of 10% fast domains, with $D_{slow}/D_{fast} = 10^{-4}$, and three different solubilities R (0.1, 10^{-2}, and 10^{-6}).

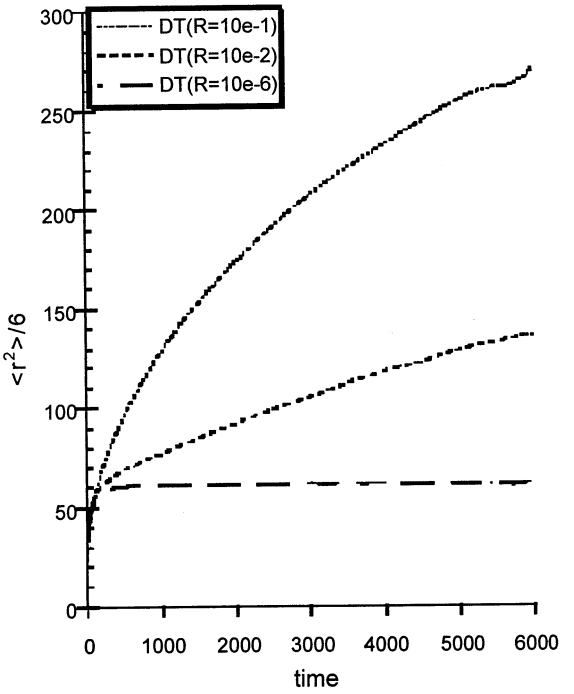

Figure 11. Average square of the distance, divided by 6, versus time for a lattice that is composed of 10% fast and 90% slow domains. The ratio of D_{slow} to D_{fast} is 10^{-4}, and three solubility ratios are shown ($R = 10^{-1}$, 10^{-2}, and 10^{-6}).

ability polymer is ~0.3, whereas the fractional free volume[17−20] associated with the larger free-volume elements is considered to be ~0.03. Thus, 10% of the free volume is associated with the large-free-volume elements. The rest of the free volume is associated with smaller-free-volume elements that are more typical of glassy polymers. The fraction of the system that is "porous" or supports fast diffusion is still not defined, because the porous domain will contain an occupied volume as well as the large-free-volume elements. It is not a true pore, because it is not free space but rather an aggregation of high-free-volume elements in a polymer matrix. If 10% of the free volume is associated with high-free-volume elements, one could assume that 10% of the total volume was porous or supported fast diffusion if both types of free-volume regions scale equivalently to give the total volume of the system. In this case, the fast-diffusion regions are well below the percolation threshold. This means that, according to the simulations, D_{app} should be qualitatively similar to restricted diffusion, which is observed if $D_{fast}/D_{slow} \geq 100$, as shown in Figure 7, rather than the apparently tortuous behavior seen in Figure 2. Positron annihilation lifetime spectroscopy data on TFE/PDD indicates a bimodal distribution of free-volume elements.[17] The smaller-free-volume elements are typical of the size seen in conventional glassy polymers, which have much slower diffusion than that observed in TFE/PDD, implying that the inequality $D_{fast}/D_{slow} \geq 100$ is reasonable.

If the diffusion is apparently tortuous, rather than apparently restricted, and the inequality is likely in place, what other factors could change the behavior to apparently tortuous? The explanation may be that the random morphology assumed in the model is not an appropriate description of this system. Computer simulation of glasses has shown strings of defects[21] and if these strings are the correct morphology for the fast-diffusion regions, diffusion behavior could be altered. A string morphology will be simulated, along with other morphologies in the future.

The other set of data is for the diffusion of diethyl ether in a blend of PEO and PMMA. PEO in this blend undergoes segmental motion on the nanosecond time scale[22−26] at room temperature well below the glass transition (70 °C). The diffusion of the diethyl ether shown in Figure 3 is rapid, with diffusion constants that are more typical of values for rubbers than for glasses. Because segmental motion for PEO is also typical of a rubber, and because rapid diffusion occurs in the blend, it is plausible that the pathway for diffusion is through the PEO-rich regions. The value of χ for this blend is small, so concentration fluctuations could be expected to be large.[27−28] Also, because D_{app} for this system is dependent on the time over which diffusion is observed, it is plausible that the PMMA regions act as barriers to diffusion. As a first approximation, one could assume that the fraction of PEO corresponds to the fraction of domains that support rapid diffusion. In the blend studied, this fraction is 20%, which is, again, below the percolation threshold. Even if the concentration of the penetrant diethyl ether is added, the fraction of fast domains would be 30%: still below the percolation limit, although now similar. However, the value of D_{app} approaches a plateau as a function of time, indicating apparently tortuous diffusion. Again, there must be better connectivity of the regions supporting fast diffusion, because the diffusion of diethyl ether in PMMA at 26 °C would be slower than the values of $10^{-7}-10^{-8}$ cm^2 s^{-1} that are observed. The PEO used in this study has a high molecular weight ($M_w = 5 \times 10^6$). The concentration fluctuations, which are reported to be 2−50 nm in size,[24] possibly are connected by the long chains. The effect of molecular weight is now being studied.

Acknowledgment. This research was conducted with the financial support of the National Science Foundation (Grant No. DMR-0209614).

References and Notes

(1) Callaghan, P. T. *Principles of Nuclear Magnetic Resonance Microscopy*; Oxford University Press: New York, 1991.

(2) Bandis, A; Inglefield, P. T.; Jones, A. A.; Wen. W.-Y. *J. Polym. Sci., Part B: Polym. Phys*. **1995**, *33*, 1495.
(3) Bandis, A.; Inglefield, P. T.; Jones, A. A.; Wen. W.-Y. *J. Polym. Sci., Part B: Polym. Phys.* **1995**, *33*, 1505.
(4) Bandis, A.; Inglefield, P. T.; Jones, A. A.; Wen. W.-Y. *J. Polym. Sci., Part B: Polym. Phys*. **1995**, *33*, 1515.
(5) Heuer, A.; Wilhelm, M.; Zimmermann, H.; Spiess H. *Phys. Rev. Lett.* **1995**, *75*, 2851.
(6) Cicerone, M. T.; Ediger, M. D. *J. Chem. Phys*. **1995**, *103*, 5684.
(7) Mitra, P. P.; Sen, P. N.; Schwartz, L. M.; Le Doussal, P. *Phys. Rev. Lett.* **1992**, *68*, 3555.
(8) Latour, L. L.; Mitra, P. P.; Kleinberg, R. L.; Sotak, C. H. *J. Magn. Reson., Ser. A* **1993**, *101*, 342.
(9) Latour, L. L.; Kleinberg, R. L.; Mitra, P. P.; Sotak, C. H. *J. Magn. Reson., Ser. A* **1995**, *112*, 83.
(10) Cicerone, M. T.; Wagner, P. A.; Ediger, M. D. *J. Phys. Chem. B* **1997**, *101*, 8727.
(11) Davis, H. T. *J. Am. Ceram. Soc.* **1977**, *60*, 499.
(12) Zwanzig, R. *Chem. Phys. Lett.* **1989**, *164*, 639.
(13) Balinov, B.; Johnsson, B.; Linse, P.; Soederman, O. *J. Magn. Reson., Ser. A* **1993**, *104*, 17.
(14) Meresi, G.; Wang, Y.; Cardoza, J.; Wen, W.-Y.; Jones, A. A.; Inglefield, P. T. *Macromolecules* **2001**, *34*, 1131.
(15) Meresi, G.; Wang, Y.; Cardoza, J.; Wen, W.-Y.; Jones, A. A.; Gosselin, J.; Azar, D.; Inglefield, P. T. *Macromolecules* **2001**, *34*, 4852.
(16) Wang, Y.; Meresi, G.; Gosselin, J.; Azar, D.; Wen, W.-Y.; Jones, A. A.; Inglefield, P. T. *Macromolecules* **2001**, *34*, 6680.
(17) Alentiev, A. Yu.; Yamploski, Yu. P.; Shantarovich, V. P.; Nemser, S. M.; Plate, N. A. *J. Membr. Sci.* **1997**, *126*, 123.
(18) Merkel, T. C.; Bondar, V.; Nagai, K.; Freeman, B. D. *Macromolecules* **1999**, *32*, 370.
(19) Bondar, V. I.; Freeman, B. D.; Yampolskii, Yu. P. *Macromolecules* **1999**, *32*, 6163.
(20) Singh, A.; Bondar, S.; Dixon, S.; Freeman, B. D.; Hill, A. J. *Polym. Mater. Sci. Eng*. **1997**, *77*, 316.
(21) Donati, C.; Douglas, J. F.; Kob, W.; Plimpton, S. J.; Poole, P. H.; Glotzer, S. C. *Phys. Rev. Lett.* **1998**, *80*, 2338.
(22) Zwada, J. A.; Fuller, Y. G. G.; Colby, R. H.; Long, T. E. *Macromolecules* **1992**, *25*, 2896.
(23) Lartigue, C.; Guillermo, A.; Cohen-Addad, J. P. *J. Polym. Sci., Part B: Polym. Phys*. **1997**, *35*, 1095.
(24) Schantz, S. *Macromolecules* **1997**, *30*, 1419.
(25) Dionisio, M.; Fernandes, A. C.; Mano, J. F.; Correia, N.; Sousa, R. C.; *Macromolecules* **2000**, *33*, 1002.
(26) Lutz, T. R.; He, Y.; Ediger, M. D.; Cao, H.; Lin, G.; Jones, A. A. *Macromolecules* **2003**, *36*, (5), 1724.
(27) Ito, H.; Russell, T. P.; Wignall, G. D. *Macromolecules* **1987**, *20*, 2213.
(28) Hopkinson, I.; Kiff, F. T.; Richards, R. W.; King, S. M.; Farren, T. *Polymer* **1995**, *36*, 3523.